International Journal of Advanced Engineering, Management and Science (IJAEMS)
Peer-Reviewed Journal
ISSN: 2454-1311 | Vol-12, Issue-2; Mar-Apr, 2026
Journal Home Page: https://ijaems.com/
DOI: https://dx.doi.org/10.22161/ijaems.122.4

A Novel Design Approach for Extended Modular Intelligent Robots

He-Rong Lee[1], Wei Lee[2], Ming-Hui Huang[3], Chun-Chi Chang[4], Ho-Sheng Chen[5*]

[1]Guangzhou Institute of Science and Technology, China
Email: chelung168@gmail.com
[4]National Taipei University of Business
Email: czoe2772@gmail.com
[2,3,5]School of Sciences, Guangdong University of Petrochem Technology (GDUPT), Maoming 525000, China
Corresponding author: Ho-Sheng Chen
Email:hschen98.tw@gmail.com

Received: 27 Jan 2026; Received in revised form: 26 Feb 2026; Accepted:28 Feb 2026; Available online: 05 Mar 2026

***Abstract*—** *This paper presents the design of a reconfigurable multi-form robot integrating UAV, hexapod biomimetic, and wheeled structures based on modular principles. The system utilizes an Arduino platform with Mega2560 microcontroller for joint motor control and a dedicated flight control module for brushless motor regulation. Physical prototyping is achieved through 3D printing technology, with detachable joint and arm structures enabling flexible module replacement and expansion. Ultrasonic sensors are incorporated to provide obstacle avoidance functionality. The proposed design demonstrates a practical approach to developing adaptable robotic systems for diverse application scenarios.*

Keywords*—** ***Modular robot; Reconfigurable mechanism; Arduino; 3D printing; Obstacle avoidance

I. INTRODUCTION

Since the 21st century, with the continuous development of science and technology, scholars at home and abroad have conducted increasingly in-depth research on robot technology. Robot technology has become a focus of attention for technology workers and is considered one of the high-tech fields that are of great significance for the development of emerging industries in the future. Robots have broad application prospects in fields such as agricultural planting, rescue and detection, military security, home services, and intelligent transportation [1,2,3,6].

In these fields, robots need to complete different types of homework tasks in dynamic, unknown, and unstructured complex environments, which puts high demands on their environmental adaptability, environmental perception, autonomous control, and human-computer interaction [4,5].

Based on the above analysis and description, this article takes a multi form robot as the research object, with six wing, six legged, and four wheeled models as the main body. Mechanical structure design, control system design, and kinematic analysis are carried out to complete corresponding simulation experiments and robot experiments, and experimental results are obtained [7-10].

II. STRUCTURAL DESIGN OF HEXACOPTER MODULE

The six-wing UAV combines the structure of a hexapod robot, featuring six propellers and six mechanical legs arranged in a hexagonal configuration [11-13]. Adjacent rotors rotate in opposite directions to counteract torque, allowing attitude control through speed adjustment. An aluminum alloy frame ensures lightweight durability and stable flight. The mechanical legs serve as

landing gear for shock absorption and enable loading, transport, and grasping functions. This design enhances performance and adaptability in hazardous environments (Figure 1) [14,15].

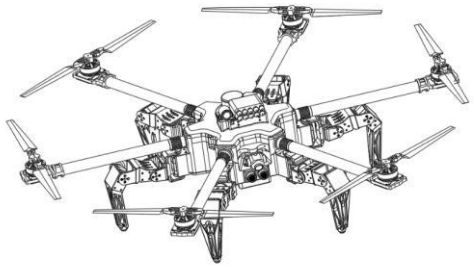

Fig.1. Structure of Unmanned Aerial Vehicle

The components n=3, 1, 2, and 3 of the mechanism are thigh, calf, and foot end components, respectively. I, II, and III are the rotating pairs of the mechanism, all of which are low pairs and do not have high pairs. According to the formula for calculating institutional degrees of freedom.

$$F = 3n - 2p_l - p_h \quad (1)$$

where n is the number of active components, p_l is the low parity of the institution; p_h is the high parity number of the institution.

Therefore, the degree of freedom F of a hexapod robot's single leg is 3, which can achieve the internal and external expansion, flexion and extension, and pitch movements of the single leg. The thigh drives the servo to rotate around the z-axis at the root joint to achieve internal and external expansion and contraction movements. Drive the servo at the calf and thigh to move in the z-axis direction to achieve pitch motion. The servo is driven to move in the y-axis direction at the foot and calf ends to achieve flexion and extension movements. At the same time, the mechanical leg uses magnets and snap fasteners at the joint between the thigh and calf joints to achieve rapid disassembly and assembly of the leg structure. The design drawings of the mechanical leg are shown in Figures 2 and 3.

Fig.2. Leg Structure

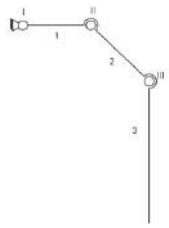

Fig.3. Mechanical principle

The front and rear wheels of the four-wheel drive car have power, and the engine output torque can be distributed on all the wheels in different proportions according to the driving road conditions to improve the driving ability of the four-wheel drive car. The four-wheel drive car controls its motion through a 24 channel development board with STM32 core as the autonomous control. The PID algorithm is used to correct the stability of the car's motion. The proportion, integral, and derivative of the deviation are linearly combined to form the control quantity of the four-wheel drive car. The control quantity is used to control the servo of the controlled object, which is the four-wheel drive car. The PID process of servo control is shown in Figure 4.

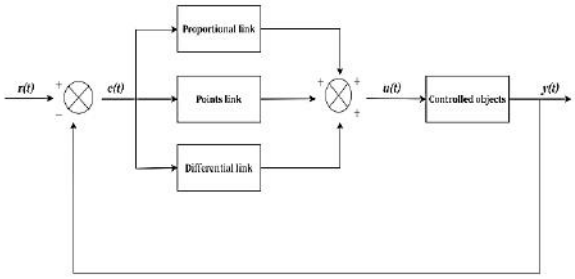

Fig.4. Servo control system of PID process

Control the aircraft's ascent, descent, rotation, and hovering movements through the thrust of six brushless motors. During the flight, the flight control system of the hexacopter drone sends commands to each electric motor to control their speed and output thrust. The combination of these instructions can enable a hexacopter drone to fly in different directions, such as forward, backward, left turn, right turn, etc., and hover in the air. For ascent and descent, the hexacopter drone achieves this by controlling the total thrust of all electric motors. When the thrust of the electric motor increases, the

aircraft will ascend; On the contrary, when the thrust decreases, the aircraft will descend. By adjusting the thrust of each electric motor, the aircraft can be deflected or rotated. During the flight, the flight control system of the hexacopter drone continuously detects the aircraft's attitude and automatically adjusts the speed of the electric motor as needed to maintain the balance and stability of the aircraft. In summary, the hexacopter drone achieves accurate control of the aircraft by controlling the speed and thrust of each electric motor, enabling operations such as flight, hovering, and turning in the air.

The rigid body model includes kinematics and dynamics. Dynamics calculates the relationship between sum force and acceleration, kinematics calculates the relationship between velocity and position, and dynamics calculates acceleration for use in kinematics [9]. Input the throttle of six motors and output the lift and torque of the body. From this, the following formula can be derived:

$$\begin{aligned} T_m\dot{\varpi}_1(t) + \varpi_1(t) &= C_m\sigma_1(t) + \varpi_m \\ T_m\dot{\varpi}_2(t) + \varpi_2(t) &= C_m\sigma_2(t) + \varpi_m \\ T_m\dot{\varpi}_3(t) + \varpi_3(t) &= C_m\sigma_3(t) + \varpi_m \\ T_m\dot{\varpi}_4(t) + \varpi_4(t) &= C_m\sigma_4(t) + \varpi_m \\ T_m\dot{\varpi}_5(t) + \varpi_5(t) &= C_m\sigma_5(t) + \varpi_m \\ T_m\dot{\varpi}_6(t) + \varpi_6(t) &= C_m\sigma_6(t) + \varpi_m \end{aligned} \quad (2)$$

From Eq. (2), can be concluded that

$$T = c_T(\varpi_1^2 + \varpi_2^2 + \varpi_3^2 + \varpi_4^2 + \varpi_5^2 + \varpi_6^2) \quad (3)$$

The resultant moment is:

$$\begin{aligned} \tau_x &= \sqrt{3}/2dc_T(-\varpi_1^2 + \varpi_2^2 + \varpi_3^2 - \varpi_4^2 - \varpi_5^2 + \varpi_6^2) \\ \tau_y &= \sqrt{3}/2dc_T(\varpi_1^2 + \varpi_2^2 + \varpi_3^2 - \varpi_4^2 - \varpi_5^2 - \varpi_6^2) \\ \tau_z &= c_M(\varpi_1^2 - \varpi_2^2 + \varpi_3^2 - \varpi_4^2 + \varpi_5^2 - \varpi_6^2) \end{aligned} \quad (4)$$

The symbols of the dynamic model and the values of the dynamic model constants are the meanings of the parameters in equations (2), (3), and (4), as shown in Table 1.

Table 1. Symbol Explanation of Dynamic Model

variable	symbol	unit
the throttle of each motor	$\boldsymbol{\sigma_1, \sigma_2, \sigma_3, \sigma_4, \sigma_5, \sigma_6}$	Normalization [0,1]
motor speed	$\boldsymbol{\varpi_1, \varpi_2, \varpi_3, \varpi_4, \varpi_5, \varpi_6}$	rad/s
lift generated	$\mathbf{F_1, F_2, F_3, F_4, F_5, F_6}$	N
induced drag generated	$\mathbf{M_1, M_2, M_3, M_4, M_5, M_6}$	N
the torque generated by the lift	$\boldsymbol{\pi_1, \pi_2, \pi_3, \pi_4, \pi_5, \pi_6}$	N·m
the reverse torque generated	$\boldsymbol{\tau_1, \tau_2, \tau_3}$	N·m
resultant moment on the axis	**89.96**	N·m
Combined lift force	**T**	N

Given a throttle, the motor will gradually reach the target speed, approximating the motor as a first-order system. Therefore, Eq. (3) shows that the stable speed is linearly related to the throttle:

$$T_m d\varpi(t)/dt + \varpi(t) = C_m\sigma(t) + \varpi_m \quad (5)$$

is equivalent to

$$\dot{\varpi}(t) = d\varpi(t)/dt = \frac{1}{T_m}\left(C_m\sigma(t) + \varpi_m - \varpi(t)\right) (6)$$

By using the above formula and Simulation model of Extended Modular Intelligent Robots based on MATLAB/Simulink to test the motor model of a six wing unmanned aerial vehicle, the conclusion can be drawn that the larger the motor time constant, the smaller the speed change, as shown in Figure 5 and 6.

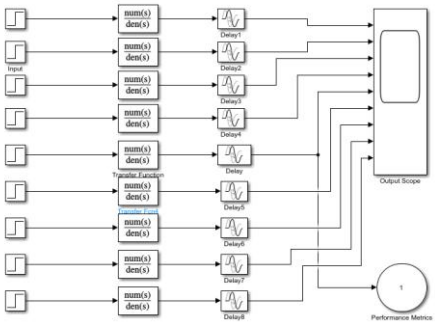

Fig.5. Simulation model of Extended Modular Intelligent Robots based on MATLAB/Simulink

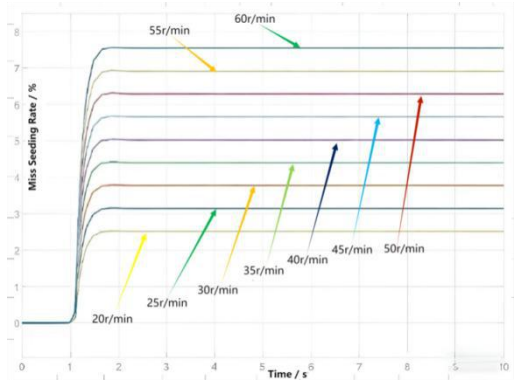

Fig.6. Test results of motor model for six wing unmanned aerial vehicle based on MATLAB

If the lift generated by a single propeller is proportional to the square of the rotational speed:

$$F = c_T \varpi^2 \tag{7}$$

The combined lift generated by the six propellers is:

$$T = c_T(\varpi_1^2 + \varpi_2^2 + \varpi_3^2 + \varpi_4^2 + \varpi_5^2 + \varpi_6^2) \tag{8}$$

The physical quantity that produces a rotational effect on an object can be divided into the moment of force on the axis and the moment of force on the point, that is, M=d × F. Among them, d is the position vector from the axis of rotation to the point of force, and F is the vector force; Torque is also a vector. According to the torque formula:

$$\begin{aligned} M_1 &= d \times F_1 \\ M_{1x} &= -\frac{\sqrt{3}}{2} dF_1 = -\frac{\sqrt{3}}{2} dc_T \varpi_1^2 \\ M_{1y} &= \frac{\sqrt{3}}{2} dF_1 = \frac{\sqrt{3}}{2} dc_T \varpi_1^2 \end{aligned} \tag{9}$$

XY axis torque:

$$\begin{aligned} \tau_x &= \frac{\sqrt{3}}{2} dc_T(-\varpi_1^2 + \varpi_2^2 + \varpi_3^2 - \varpi_4^2 - \varpi_5^2 + \varpi_6^2) \\ \tau_y &= \frac{\sqrt{3}}{2} dc_T(\varpi_1^2 + \varpi_2^2 + \varpi_3^2 - \varpi_4^2 - \varpi_5^2 - \varpi_6^2) \\ \tau_z &= c_M(\varpi_1^2 - \varpi_2^2 + \varpi_3^2 - \varpi_4^2 + \varpi_5^2 - \varpi_6^2) \end{aligned} \tag{10}$$

Drones should be studied for dynamics based on dynamic coordinates. According to the Euler equation of a rigid body, the absolute derivative in dynamic coordinates can be expressed as: $\sum M^b = I\dot{W}^b + W^b \times (IW^b)$, where (p, q, r are the roll, pitch, and yaw velocities in the body coordinate system, respectively):

$$I = \begin{bmatrix} I_x & 0 & 0 \\ 0 & I_y & 0 \\ 0 & 0 & I_z \end{bmatrix} \tag{11}$$

According to the above equation:

$$\begin{aligned} M_x &= I_x \dot{p} + (I_z - I_y)qr \\ M_y &= I_y \dot{q} + (I_x - I_z)pr \\ M_z &= I_z \dot{r} + (I_y - I_x)pq \end{aligned} \tag{12}$$

By simplifying, we can obtain:

$$\begin{bmatrix} M_{Tx} \\ M_{Ty} \\ M_{Fz} \end{bmatrix} = \begin{bmatrix} l(F_6 - F_4 - F_2) \\ l(F_5 - F_3 - F_1) \\ -M_{D1} + M_{D2} - M_{D3} + M_{D4} - M_{D5} + M_{D6} \end{bmatrix} = \begin{bmatrix} lb(\Omega_6^2 - \Omega_4^2 - \Omega_2^2) \\ lb(\Omega_5^2 - \Omega_3^2 - \Omega_1^2) \\ d(-\Omega_1^2 + \Omega_2^2 - \Omega_3^2 + \Omega_4^2 - \Omega_5^2 + \Omega_6^2) \end{bmatrix} \tag{13}$$

where, b is the rotor lift coefficient, d is the rotor drag coefficient, and represents the rotor speed.

III. ROBOT PROGRAMMING AND SIMULATION

Zide is a graphical programming tool for multi-channel servos dominated by PWM signals. The upper computer can directly use a 24 channel servo control board to write data for the 18 motion servos of the robot, and can group the written data into action groups. The Zide upper computer page is shown in Figure 7, which saves a lot of workload and time for subsequent programming work.

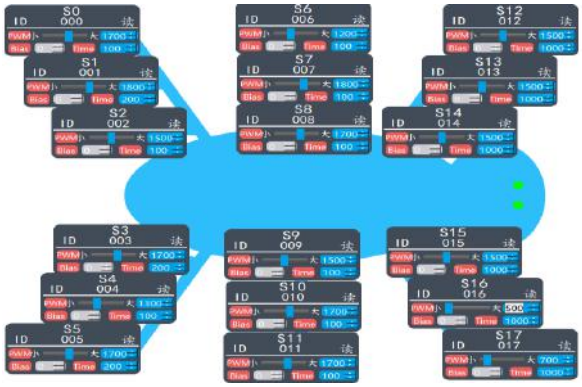

Fig.7. Zide upper computer interface diagram

We will label the 18 servos of the robot according to S0-S17, and classify these labels according to the six legs of the robot. Use SO-S2 as leg 1, S3-S5 as leg 2, S6-S8 as leg 3, S9-S11 as leg 4, S12-S14 as leg 5, and S15-S17 as leg 6. The driving motor of the wheels uses a 360 ° servo motor, which is controlled by

PWM signals. The servo motors of the four wheels are calibrated as S1-S4 as shown in Figure 8. S0 is the left front wheel, S2 is the right front wheel, S1 is the left rear wheel, and S3 is the right rear wheel. The actions of the car are divided into four parts: forward, rear wheel, left turn, and right turn.

Fig.8. Arrangement diagram of small car servo motor

Taking forward and left turn actions as an example, the data of the car's actions are shown in Table 2

Table 2. Data of small car action servo

	S_0	S_1	S_2	S_3
forward	2500	2500	2500	2500
turn left	50	50	2500	2500

First, install the servo into the installation slots of each leg, and then connect the three joints into the main body using the servo disc and nuts. Cut the carbon brazing tube into six sections and connect them to each other through carbon tube connection blocks and motor mounts. Before installing the ultrasonic sensor into the main body, as shown in Figure 9

Fig.9. The Extended Modular Intelligent Robots

IV. CONCLUSION

This article proposes a design and manufacturing method for an extended class multimodal robot, which integrates three modules: hexapod robot, hexacopter drone, and four-wheel cart. By designing a detachable structure, different forms can be switched, and a six legged leg structure and a wheeled structure for the car can be designed using Solid Works. And the corresponding driving electrical components were selected. The designed parts were produced using 3D printing technology. Then, FDM 3D printer technology was used to print and assemble the parts. In terms of control, use Arduino and Linkboy platforms to write relevant posture and motion control programs, use Arduino 2560 and 24 channel servo control board, and combine with ultrasonic obstacle avoidance module, relay, lighting, etc. The robot action group was programmed and debugged using Zide servo programming software, and the flight power parameters of the brushless motor were debugged using flight control parameter tuning software. Finally, the robot's form was assembled and tested.

REFERENCES

[1] Wang Yu. (2021). Gait planning and control system design of hexapod robot (Master's thesis). Hubei University of Technology. DOI:10.27131/d.cnki.ghugc.2021.000155.

[2] Liu Yan, Zheng Luying, Sun Haoyang, Ma Bingran, Zhang Shenghan. (2018). Motion analysis of hexapod robot under triangular gait. Journal of Qingdao University, 33(03), 38-42+46. DOI:10.13306/j.1006-9798.2018.03.007.

[3] Sun Xun. (2022). Research on gait design of hexapod robot in complex slope environment (Master's thesis). Harbin University of Science and Technology. DOI:10.27063/d.cnki.ghlgu.2022.001126.

[4] Ding Kai. (2016). Research on bionic locomotion gait planning and control system of hexapod robot (Master's thesis). Southeast University.

[5] Chen Rui, Chen Nanxing, Huang Wenjun, Wang Zhanhao, Ma Changyun. (2020). Hexapod robot applied to post-disaster rescue and patrol measurement. Electronics World, (09), 132-133. DOI:10.19353/j.cnki.dzsj.2020.09.070.

[6] Fan Dingjia. (2019). Design of flight control system for six-rotor UAV (Master's thesis). North University of China.

[7] Yang Jiankang. (2020). Design and implementation of grasping system for rotor UAV (Master's thesis). Nanjing University of Information Science and Technology. DOI:10.27248/d.cnki.gnjqc.2020.000378.

[8] Qiu Pengrui. (2022). Research on vision-based pose estimation and flight control of quadrotor UAV (Master's thesis). Kunming University of Science and Technology. DOI:10.27200/d.cnki.gkmlu.2022.000029.
[9] Shao Linwen, Liao Fang, Ding Liming, Shu Wei, He Zhiqian. (2021). PID simulation design of quadrotor UAV flight control based on MATLAB. Shanxi Electronic Technology, (05), 43-46.
[10] Zhang Xuejin, Qin Yi. (2015). Research and application of four-wheeled car based on Arduino. Today's Electronics, (06), 57-59.
[11] Li Zhiqiang, Kang Qinqing, Xiao Yuliang, Li Bengao, Huang Ming, Wang Dongtao. (2022). Design and implementation of intelligent car based on Arduino. Wireless Internet Technology, 19(16), 43-46.
[12] Fu Xiaoyun. (2021). Design and development of intelligent obstacle avoidance car based on Arduino typical sensors. Precision Manufacturing and Automation, (02), 25-29. DOI:10.16371/j.cnki.issn1009-962x.2021.02.006.
[13] Jin Ma, Ding Liang, Gao Haibo, Su Yang, Zhang Pinjia. (2023). Dynamics modeling and simulation of a hexapod robot with a focus on trajectory prediction. Journal of Intelligent & Robotic Systems, 108(1).
[14] Yao Shun, Yao Yanan, Liu Ran, Liu Chao. (2022). A portable off-road crawling hexapod robot. Journal of Field Robotics, 39(6).
[15] Wangyue Di, Xin Tong, Zhigang Li. (2022). Tracking control of the six-rotor UAV with input dead-zone and saturation. IAENG International Journal of Applied Mathematics, 52(4).